

Spin-wave propagation in a microstructured magnonic crystal

A. V. Chumak,^{1,*} P. Pirro,¹ A. A. Serga,¹ M. P. Kostylev,² R. L. Stamps,² H. Schultheiss,¹ K. Vogt,¹ S. J. Hermsdoerfer,¹ B. Laegel,¹ P. A. Beck,¹ and B. Hillebrands¹

¹*Fachbereich Physik, Nano+Bio Center, and Forschungszentrum OPTIMAS, Technische Universität Kaiserslautern, 67663 Kaiserslautern, Germany*

²*School of Physics, University of Western Australia, Crawley, Western Australia 6009, Australia*
(Dated: October 29, 2018)

Transmission of microwave spin waves through a microstructured magnonic crystal in the form of a permalloy waveguide of a periodically varying width was studied experimentally and theoretically. The spin wave characteristics were measured by spatially-resolved Brillouin light scattering microscopy. A rejection frequency band was clearly observed. The band gap frequency was controlled by the applied magnetic field. The measured spin-wave intensity as a function of frequency and propagation distance is in good agreement with a model calculation.

Magnonic crystals (MCs) operate with spin waves (SW) in the microwave frequency range [1, 2, 3, 4, 5, 6, 7, 8, 9, 10, 11, 12] and are the magnetic counterpart of photonic and sonic crystals. The greatest success in MC making has been achieved with yttrium-iron-garnet (YIG) film based structures due to the extremely small magnetic loss [1, 2, 3, 4, 5]. However, comparatively large sizes of these devices (hundreds of microns) and the incompatibility of the YIG film growing process with modern CMOS technology inhibit their wide practical use. Applications in microelectronics require downscaling to sub-micron sizes and a replacement of YIG films by thin ferromagnetic metallic layers.

Previous studies of metal film based microstructured magnonic crystals (micro-MCs) were mostly focused on their thermal SW spectrum [6, 7, 8], or were purely theoretical [9, 10, 11, 12]. Here we report on the experimental observation and characterization of spin-wave propagation in a metal micro-MC.

To ensure SW propagation the crystal was fabricated as a SW-waveguide made from a permalloy (Py) stripe with a periodically varying width. This concept was suggested in theoretical works done in the group of S. K. Kim

[9, 10]. However, the proposed feature sizes of the order of nanometers, which were chosen due to size limitation in computer simulation, and consequently practically vanishing SW group velocities make the original structure very difficult to fabricate and test at the current level of technology. In this work we have modified the original waveguide geometry such that it is now supporting propagation of spin waves over distances of tens of micrometers. Towards this end we have increased the waveguide thickness (the SW group velocity is roughly proportional to this dimension) and applied a bias magnetic field across the waveguide (see Fig. 1) to form conditions for propagation of guided Damon-Eschbach surface spin waves [13]. In in-plane magnetized metallic samples with a high-magnetic moment these waves have the highest group velocities. Furthermore, for this magnetization direction the waveguide's internal magnetic field is strongly inhomogeneous due to static demagnetization. As a result, in addition to periodical variation of the waveguide width, periodical modulation of the internal bias field takes place in this geometry. This additionally increases the efficiency of spin-wave reflection.

Electron beam lithography, molecular beam epitaxy, and lift-off process were used to fabricate the magnonic crystal in the form of a notched permalloy stripe on thermally oxidized Si(001) substrate (see Fig. 1). The width of the 40 nm thick Py ($\text{Ni}_{81}\text{Fe}_{19}$) stripe varies periodically between $w_0 = 2.5 \mu\text{m}$ and $w_1 = 1.5 \mu\text{m}$. The length of the $2.5 \mu\text{m}$ -wide sections is $0.75 \mu\text{m}$ and the length of the $1.5 \mu\text{m}$ -wide sections ("notches") is $0.25 \mu\text{m}$. This forms a magnonic crystal with a lattice constant $a = 1 \mu\text{m}$. As a reference a second waveguide with a uniform $w_0 = 2.5 \mu\text{m}$ width was also patterned on the same substrate $6 \mu\text{m}$ apart from the magnonic crystal (see Fig. 1).

Spin waves are excited by the microwave Oersted field created by a 500 nm thick and $w_a = 1 \mu\text{m}$ -wide copper antenna, which is placed across the both Permalloy waveguides (see Fig. 1). In order to detect spin waves the space-resolved Brillouin light scattering microscopy is used [14]: a focused laser beam probes spin waves with

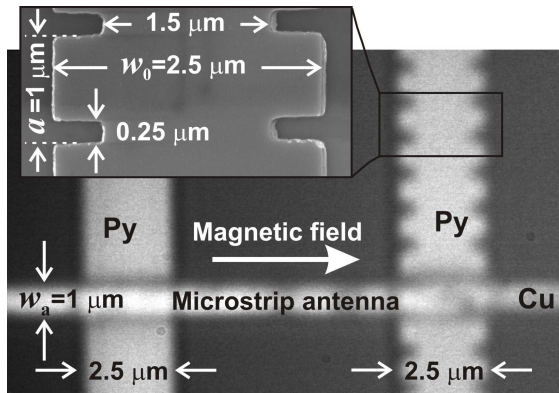


FIG. 1: Scanning electron microscopy and optical images of the structure under study. The uniform reference waveguide is shown on the left and the magnonic crystal on the right.

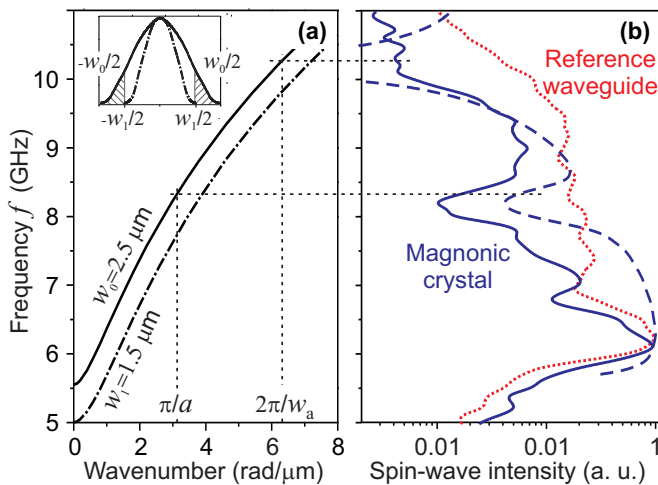


FIG. 2: (Color online). (a) Calculated SW dispersion curves for uniform waveguides with $w_0 = 2.5 \mu\text{m}$ (solid line) and $1.5 \mu\text{m}$ (dash-dotted line). The inset shows profiles of the fundamental width modes in uniform waveguides of different widths. (b) Normalized SW intensity measured at the distance $x = 8 \mu\text{m}$ from the antenna versus the applied frequency. Solid line – the magnonic crystal; dotted line – the reference waveguide. Dashed line represents the calculation for the magnonic crystal. For both panels the bias magnetic field and the saturation magnetization are 500 Oe and $M_s = 770 \text{ G}$.

a spatial resolution of 250 nm and a frequency resolution of 300 MHz [14, 15, 16].

The calculated dispersion for the lowest (fundamental) width mode of a $w_0 = 2.5 \mu\text{m}$ -wide uniform waveguide is shown in Fig. 2(a) as solid line. For comparison, in this panel we also show the dispersion for a $1.5 \mu\text{m}$ -wide uniform waveguide which corresponds to the narrow sections of the magnonic crystal. The calculation was carried out by numerically solving the integro-differential equation derived in Ref. [13]. Note, that this calculation takes into consideration the inhomogeneity of the internal static magnetic field and the static magnetization which is also responsible for the bell-shaped transverse profile of the fundamental mode (see, the inset in Fig. 2).

The experimentally measured SW intensity for the reference waveguide is shown in Fig. 2(b) (dotted line) as a function of the applied microwave frequency. The maximum intensity corresponds to spin waves with wavenumbers slightly larger than $k = 0$ because of the highest excitation efficiency and the highest SW group velocity. With increasing frequency (and increasing spin-wave wavenumber, respectively) the excitation efficiency drops [16]. For the used antenna it gets close to zero above 11 GHz. A weak oscillatory intensity variation with frequency can be understood as beating of the fundamental width mode with the third one, which is also excited by the antenna but less efficiently [15, 17].

Solid line in Fig. 2(b) shows the measured SW inten-

sity for the magnonic crystal. A pronounced rejection band (where spin waves are not allowed to propagate) is clearly observed for frequencies close to 8 GHz. One can see that the rejection frequency is slightly shifted down with respect to the frequency expected from the simple Bragg analysis of the SW dispersion for the uniform $2.5 \mu\text{m}$ -wide waveguide ($k_{\text{rej1}} = \pi/a = 3.14 \text{ rad}/\mu\text{m}$). We suppose that this is due to inhomogeneity of the internal magnetic field within the crystal. The decrease in the internal field between the opposite notches shifts the dispersion curve downwards in frequency. As a result the condition $k_{\text{rej1}} = \pi/a$ is fulfilled for a smaller frequency value. It is worth noting that the rigorously calculated SW intensity, which is also shown in Fig. 2(b), is in good agreement with the experiment. The second rejection band $k_{\text{rej2}} = 2\pi/a = 6.28 \text{ rad}/\mu\text{m}$ is visible in Fig. 2(b) as well. However, it is not well pronounced because k_{rej2} coincides with the edge of the antenna excitation band $k_{\text{max}} = 2\pi/w = 6.28 \text{ rad}/\mu\text{m}$.

Scattering of spin waves from an array of notches on a stripe waveguide is described by an equation similar to Eq. (5) in Ref. [18]:

$$\hat{\chi}(\mathbf{r})\mathbf{h}_d(\mathbf{r}) + \int_S \hat{G}_{\text{exc}}(\mathbf{r} - \mathbf{r}')\hat{\nu}(\mathbf{r}')\mathbf{h}_d(\mathbf{r}')d^2\mathbf{r}' = \mathbf{m}_0(\mathbf{r}), \quad (1)$$

where \mathbf{h}_d is the total dynamic dipole field of the incident and the scattered spin waves, $\hat{\nu}(\mathbf{r}) = (\hat{\chi}_0(\mathbf{r})^{-1}\hat{\chi}(\mathbf{r}) - \hat{I})$, $\hat{\chi}$ is the microwave magnetic permeability tensor which is position dependent through the nonuniformity of the internal static magnetic field and the static magnetization, $\hat{\chi}_0$ is its value for the respective uniform waveguide of the width w_0 , \hat{G}_{exc} is the Green's function of excitation of waves in this waveguide, \mathbf{m}_0 is the amplitude of the spin wave with a wavenumber k incident on the notch array, and \hat{I} is the identity tensor. This equation allows an analytical solution in the First Born Approximation (FBA) [5, 18]. From this analytic solution it can be shown that the depth of the rejection minima is proportional to the total dipole energy E of the incident spin wave contained in the waveguide cross-section which is cut out by the notches (shaded area in the inset in Fig. 2). Figuratively, part of the spin-wave energy incident on a pair of notches is reflected because the SW width profile does not fit into the narrow waveguide section. The reflection grows faster than linearly with the notch depth, as E grows with the size of the dashed area in the inset. In particular, one may expect a negligible rejection when the notch depth is smaller than the size of the demagnetized area at the edge of the uniform waveguide. This assumption is confirmed by our measurements on a different micro-MC having 250 nm-deep notches.

To get a closer insight into the wave scattering mechanisms we performed a simulation based on a phenomenological approach from [2, 19]. For this purpose we consider the micro-MC as a periodical sequence of sections of regular transmission lines with different prop-

agation constants (different k -values) for the same carrier frequency. The rejection coefficient at the junction of wider-to-narrower waveguide can then be written as $\Gamma_{0-1} = (k_1 - k_0)/(k_1 + k_0) + \Gamma'$, where k_0 and k_1 are the wavenumbers for w_0 -wide and w_1 -wide waveguide sections, respectively [19]. As it was mentioned above, the spin wave is scattered back not only due to the difference in k , which is accounted by first summand Γ_{0-1} , but also because its initial transverse profile does not fit into the width w_1 . To account for this additional reflection mechanism we phenomenologically introduce Γ' . The rejection coefficient for the waveguide junction narrower-to-wider contains only one term $\Gamma_{1-0} = -(k_1 - k_0)/(k_1 + k_0)$.

The theoretical dependence of the SW intensity on the applied frequency is shown in Fig. 2(b) with a dashed line. It was calculated as $(F(k_0)/|T_{11}|)^2$, where $F(k_0) \propto \sin(k_0 \cdot w_a/2)/k_0$ is the efficiency of the antenna excitation. T_{11} is the element (1,1) of the MC transmission matrix (see [2, 19]) which includes Γ_{1-0} , Γ_{0-1} , and the experimentally measured spatial SW damping corresponding to a Gilbert damping parameter $\alpha \approx 0.007$ [20]. This best fit is obtained for $\Gamma' = 0.12$. It means that 12 percent of incident beam energy is reflected back due to the geometrical mismatch between the waveguide sections. We should also emphasize that the reflection caused by the change of the SW wavenumbers is of the same order.

The experimentally measured transmission characteristic for the micro-MC is shown in Fig. 3(a) for different bias magnetic fields. Good agreement between the theory and the experiment is seen. The first rejection band is clearly visible for all the fields higher than 150 Oe. This value corresponds to the minimum field one has to apply in order to saturate the magnonic crystal. One also sees that variation of the applied bias magnetic field in the range from 150 Oe to 700 Oe makes it possible to control the band gap frequency in the range from 6.5 to 9 GHz.

Figure 3(b) shows the SW intensity for both the magnonic crystal and the reference waveguide as a function of the spin-wave propagation distance ($x = 0$ corresponds to the edge of the antenna) [21]. The intensity was measured in the middle of the stripes along their longitudinal axes. The oscillations of the SW intensities with x can be interpreted as the spatial beating of different waveguide width modes [15]. The dependence obtained in the transmission band of the micro-MC is very similar to the one from the reference waveguide. This fact proves the ability of practically undisturbed SW propagation in the metal waveguide with strongly damaged edges. At the same time spin waves in the band gap undergo pronounced resonant scattering. It results in an intensity which is ten times smaller than that for the reference sample after passing eight periods of the structure.

In conclusion, a micro-sized magnonic crystal operational at microwave frequencies has been fabricated in the form of a notched permalloy waveguide. Formation of

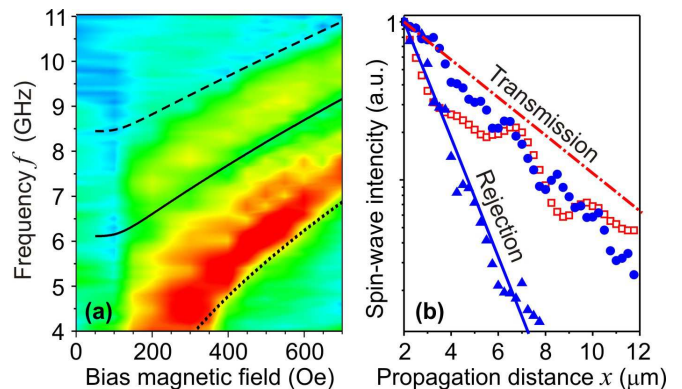


FIG. 3: (Color online). (a) Measured spin-wave intensity as a function of frequency and bias magnetic field. Logarithmic scale is used. Red color corresponds to the maximum and blue color to the minimum SW intensity. The dotted line shows the calculated frequency for the zero SW wavenumber; solid and dashed lines mark the frequencies for the first rejection band (k_{rej1}) and for the limit of antenna excitation (k_{max}), respectively. Distance from the antenna edge $x = 8 \mu\text{m}$. (b) Measured spin-wave intensity as a function of propagation distance x . Filled triangles – magnonic crystal rejection band (the applied frequency is 8.1 GHz); filled circles – magnonic crystal transmission band (8.9 GHz); opened squares – reference waveguide (8.1 GHz). Solid and dash-dotted lines show the calculation for the magnonic crystal and the reference waveguide (8.1 GHz). Bias magnetic field is 500 Oe.

pronounced magnonic band gaps was observed. They are seen as considerable decrease in SW transmission caused by the resonant backscattering from a periodical lattice. The band gap frequency can be tuned in the range from 6.5 to 9 GHz by varying the applied magnetic field.

Financial support by the DFG SE 1771/1-1, Australian Research Council, and the University of Western Australia is acknowledged.

* Electronic address: chumak@physik.uni-kl.de

- [1] S. L. Vysotskii, S. A. Nikitov, and Yu. A. Filimonov, JETP **101**, 636 (2005).
- [2] A. V. Chumak, A. A. Serga, B. Hillebrands, and M. P. Kostylev, Appl. Phys. Lett. **93**, 022508 (2008).
- [3] A. V. Chumak, A. A. Serga, S. Wolff, B. Hillebrands, and M. P. Kostylev, Appl. Phys. Lett. **94**, 172511 (2009).
- [4] A. B. Ustinov, N. Yu. Grigoreva, and B. A. Kalinikos, JETP Lett. **88**, 31 (2009).
- [5] A. V. Chumak, T. Neumann, A. A. Serga, B. Hillebrands, and M. P. Kostylev, J. Phys. D: Appl. Phys. **42**, 205005 (2009).
- [6] G. Gubbiotti, S. Tacchi, G. Carlotti, N. Singh, S. Goolaup, A. O. Adeyeye, and M. Kostylev, Appl. Phys. Lett. **90**, 092503 (2007).
- [7] M. Kostylev, P. Schrader, R. L. Stamps, G. Gubbiotti, G. Carlotti, A. O. Adeyeye, S. Goolaup, and N. Singh, Appl. Phys. Lett. **92**, 132504 (2008).

- [8] Z. K. Wang, V. L. Zhang, H. S. Lim, S. C. Ng, M. H. Kuok, S. Jain, and A. O. Adeyeye, *Appl. Phys. Lett.* **94**, 083112 (2009).
- [9] K. S. Lee, D. S. Han, and S. K. Kim, *Phys. Rev. Lett.* **102**, 127202 (2009).
- [10] S. K. Kim, K. S. Lee, and D. S. Han, *Appl. Phys. Lett.* **95**, 082507 (2009).
- [11] V. V. Kruglyak, R. J. Hicken, A. N. Kuchko, and V. Y. Gorobets, *J. Appl. Phys.* **98**, 014304 (2005).
- [12] M. Krawczyk and H. Puzkarski, *Phys. Rev. B* **77**, 054437 (2008).
- [13] M. P. Kostylev, G. Gubbiotti, J.-G. Hu, G. Carlotti, T. Ono, and R. L. Stamps, *Phys. Rev. B*, **76**, 054422 (2007).
- [14] V. E. Demidov, S. O. Demokritov, B. Hillebrands, and M. Laufenberg, *Appl. Phys. Lett.* **85**, 2866 (2004).
- [15] V. E. Demidov, S. O. Demokritov, K. Rott, P. Krzysteczko, and G. Reiss, *Appl. Phys. Lett.* **91**, 252504 (2007).
- [16] V. E. Demidov, M. P. Kostylev, K. Rott, P. Krzysteczko, G. Reiss, and S. O. Demokritov, *Appl. Phys. Lett.* **95**, 112509 (2009).
- [17] A. A. Serga, M. P. Kostylev, and B. Hillebrands, *Phys. Rev. Lett.* **101**, 137204 (2008).
- [18] M. P. Kostylev, A. A. Serga, T. Schneider, T. Neumann, B. Leven, B. Hillebrands, and R. L. Stamps, *Phys. Rev. B* **76**, 184419 (2007).
- [19] A. V. Chumak, A. A. Serga, S. Wolff, B. Hillebrands, and M. P. Kostylev, *J. Appl. Phys.* **105**, 083906 (2009).
- [20] S. S. Kalarickal, P. Krivosik, M. Wu, C. E. Patton, M. L. Schneider, P. Kabos, T. J. Silva, and J. P. Nibarger, *J. Appl. Phys.* **99**, 093909 (2006).
- [21] The data for $x < 2 \mu\text{m}$ were removed from the picture because magnetization dynamics in this area is predominantly not a propagating wave but represents a near antenna field.